

MULTI-WAVE AND FULL-WAVEFORM INVERSION IN SOUTHERN OMAN

S. Masclet¹, G. Bouquard¹, H. Prigent¹

¹ CGG

Summary

With a shallow anhydrite layer, strong multiples and converted wave contamination, Southern Oman represents an outstanding challenge for land velocity model building and imaging. While acoustic land full-waveform inversion (FWI) has proved successful on new broadband datasets in Northern Oman, no successful application has been reported for Southern Oman. We show here that the challenge of acoustic FWI in South Oman can be overcome using a dedicated workflow combining Multi-Wave Inversion (MWI) and multi-Dimensional Optimal Transport FWI (multiD OT-FWI). The key component of the workflow is the very near surface characterization provided by surface wave dispersion curves, which allows delineation of the Rus layer in the initial FWI model. MultiD OT-FWI is then used to mitigate amplitude issues in the presence of short period multiples and reduce cycle skipping beyond the depth of penetration of diving waves.

Introduction

Shallow stratigraphy in Southern Oman is characterized by the presence of an anhydrite layer and carbonate sequences with high velocities overlying a lower velocity clastic series. This geological sequence yields a shallow sharp velocity inversion and a strong curtain of multiples, causing seismic imaging to be particularly challenging in the region. While characterizing the near surface is an obvious condition to correctly imaging deeper targets, it also appears to be a key step to successful full-waveform inversion (FWI) application. We propose here a Multi-Wave Inversion (MWI) and multi-Dimensional Optimal Transport FWI (multiD OT-FWI) workflow to build a reliable velocity model and illustrate our method on a wide azimuth (WAZ) broadband high density dataset.

Geological context and Geophysical challenges

The Early Eocene witnessed persistent and widespread evaporite precipitation identified as the Rus formation (*Figure 1a*). Without any significant later sedimentation, this anhydrite layer outcrops in many areas of the Arabian peninsula (*Figure 1b*), particularly in the South of Oman where we observe considerable deposits.

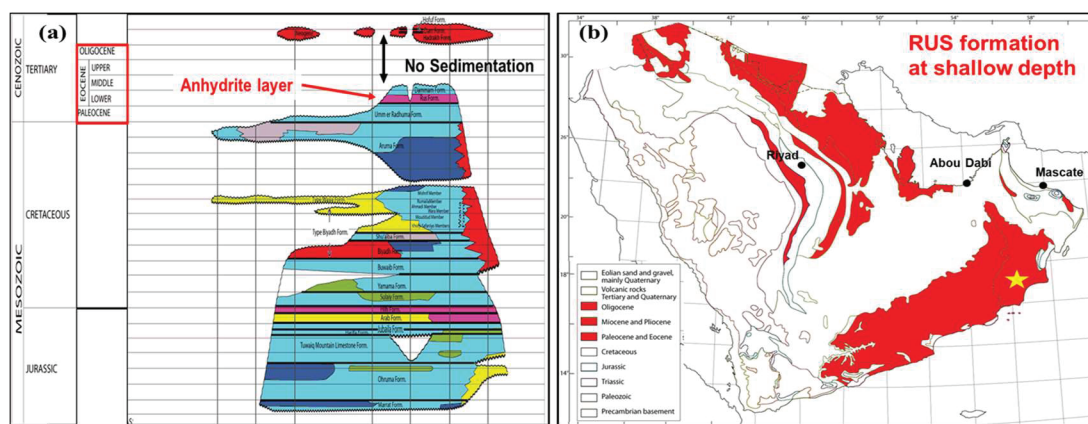


Figure 1 (a) Age relationships of Saudi Arabian sedimentary rocks. The Outcrop sequence shows no sedimentation after deposition of the anhydrite layer (Rus). (b) Geological map of the Arabian Peninsula – in red is where the Rus layer can be potentially found at shallow depths.

The Rus formation causes a sharp velocity inversion in the near surface (*Figure 2a*) which makes seismic imaging particularly difficult. Underneath the Rus layer, the Natih Formation consists of a 400 meter thick carbonate sequence with strong reflectivity and high velocity contrasts overlying a lower reflectivity clastic series with weak impedance contrasts and lower velocities.

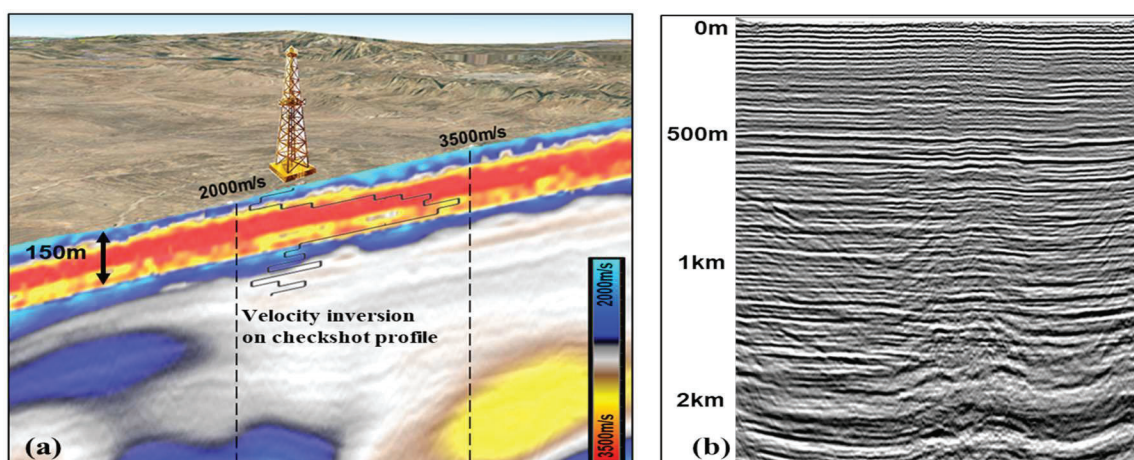


Figure 2 (a) Illustration showing shallow velocity inversion on both the check-shot profile and velocity model obtained by MWI. (b) Example of an imaged stack in Southern Oman showing strong multiple contamination.

This geological setting yields strong contamination of the lower unit by highly energetic interbed multiples generated within the upper unit by veiling the primaries with a curtain of multiples (*Figure 2b*). These multiples have the same or higher apparent velocity than the primaries, making discrimination by normal move out very challenging.

Near surface characterization by Multi-Wave Inversion and its impact on FWI

Despite the recent advances in land depth imaging technology (Sedova et al., 2017), the known sharp velocity inversion described previously is extremely difficult to be captured, with either reflection-based or diving-wave inversion methods. Reflection tomography suffers from insufficient near angles and poor signal-to-noise ratio (SNR) while refraction tomography and diving-wave FWI are impeded by illumination gaps in the presence of strong velocity inversions (*Figure 4a*). In this geological context, Masclet et al. (2019) have shown that MWI approach proposed by Bardainne (2018) leads to an accurate estimate of the very near subsurface model. However, using a proper data driven analysis based on machine-learning, the surface wave dispersion curves allow the detection of an anhydrite layer with its subsequent velocity inversion (*Figure 2a*). The lateral resolution obtained in the shallow P-wave velocity model with MWI is definitely higher than the resolution obtained through First Break (FB) tomography (*Blue arrow pointing at shallow Karst formation in Figure 3a, 3b*). The imaging of the shallow formations, including fine geological features, is greatly improved with MWI (*Figure 3c, 3d*).

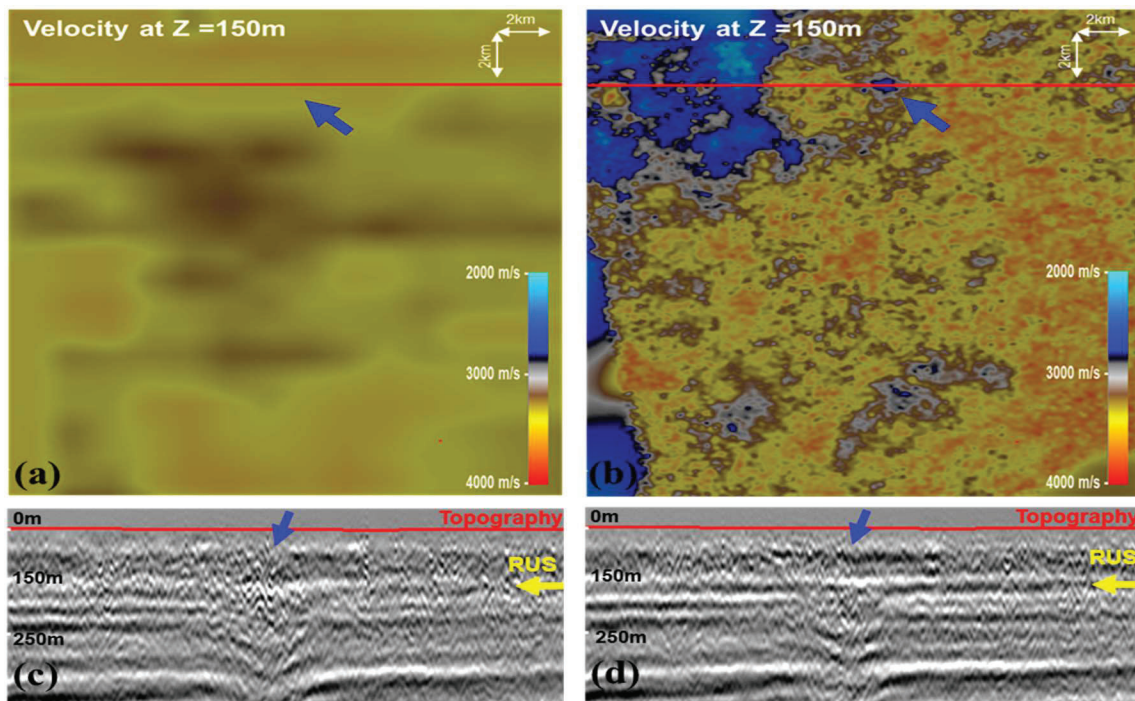


Figure 3 Depth slice through the velocity model at 150 m below topography: (a) after conventional first break tomography, and (b) after MWI. Depth migrated image of near common offset vector located at the red line using velocity model obtained through: (c) FB tomography, and (d) MWI.

Conversely, depending on the minimum pick-able frequency of the Rayleigh waves, MWI can only provide a limited depth update ($\sim 350\text{m}$ below topography in our case), which makes impossible to update the full depth range where reflection tomography fails. Despite the unfavourable conditions described by Perez Solano and Plessix, (2019), acoustic FWI offers a cost effective solution for large-scale production projects. We suggest that the preliminary pass of MWI can strongly reduce the risk of cycle skipping in acoustic FWI by correctly inserting key multiple generators at the Rus interfaces. Two FWI updates, with and without preliminary MWI (*Figure 4c and 4a, respectively*), were run in parallel. The resulting velocity models exhibit more lateral stability and sharper vertical velocity contrasts when MWI is used in advance. The corresponding migrated sections also feature improved lateral continuity (*Figure 4d, 4b*).

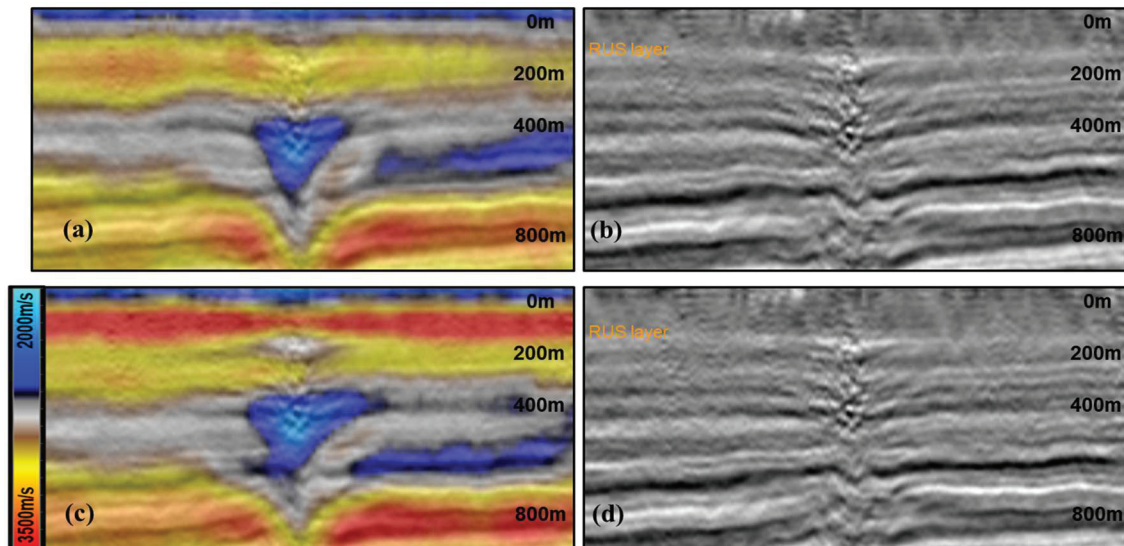


Figure 4 P-wave velocity model and corresponding reverse time migrated stack image (RTM): (a & b) after 7 Hz Least Square FWI without MWI model, (c & d) after 7 Hz Least Square FWI with MWI model.

Optimal Transport FWI

With a maximum acquired offset of 12 km, our current dataset allows us to run diving-wave FWI over a 2 km depth section, well beyond the Rus layer (Figure 5). At all levels, the strong short-period internal multiple contamination presents a challenge for conventional acoustic FWI due to the increased risk of inaccurate forward modelled amplitudes (Perez Solano and Plessix, 2019).

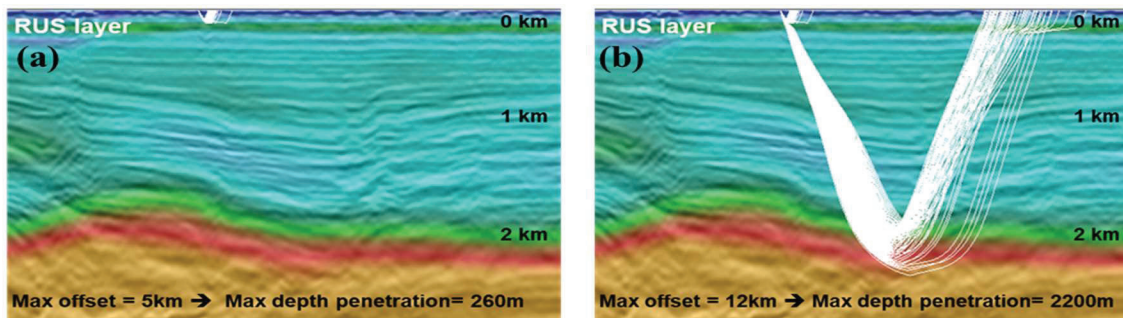


Figure 5 Diving-wave ray-tracing analysis performed on the initial velocity model including MWI shallow velocities (Rus layer) with: (a) 5 km maximum offset, and (b) 12 km maximum offset.

The multiD OT-FWI scheme, proposed by Metivier et al. (2016), can mitigate against these amplitude inaccuracies due to its reduced sensitivity to amplitude variation. Successful examples have been reported in Northern Oman where OT-FWI significantly improved the inversion stability over conventional Least Square (LS) FWI (Sedova et al., 2019; Hermant et al., 2020, “Imaging Complex Fault Structures On-shore Oman Using Optimal Transport Full Waveform Inversion”, submitted to 82nd EAGE Conference and Exhibition), especially when reflections are included to update below the diving wave maximum penetration depth. With this Southern Oman example, we also observe the benefits of multiD OT-FWI in the presence of short period internal multiples. Figure 6 highlights the gradual improvement of the velocity model and the respective migrated section transitioning from multi-layered non-linear slope tomography to 7 Hz LS-FWI and then 7 Hz OT-FWI. The turtle-back structure, where conflicting dips on the image clearly illustrate the presence of internal multiples, gains coherency with the FWI velocity updates. However, some velocity inconsistencies, possibly induced by multiple related cycle skipping, remain in the LS-FWI model (blue arrow on Figure 6b) The OT-FWI addresses these anomalies and greatly improves the deeper update where the mute has been opened to allow reflections in the inversion.

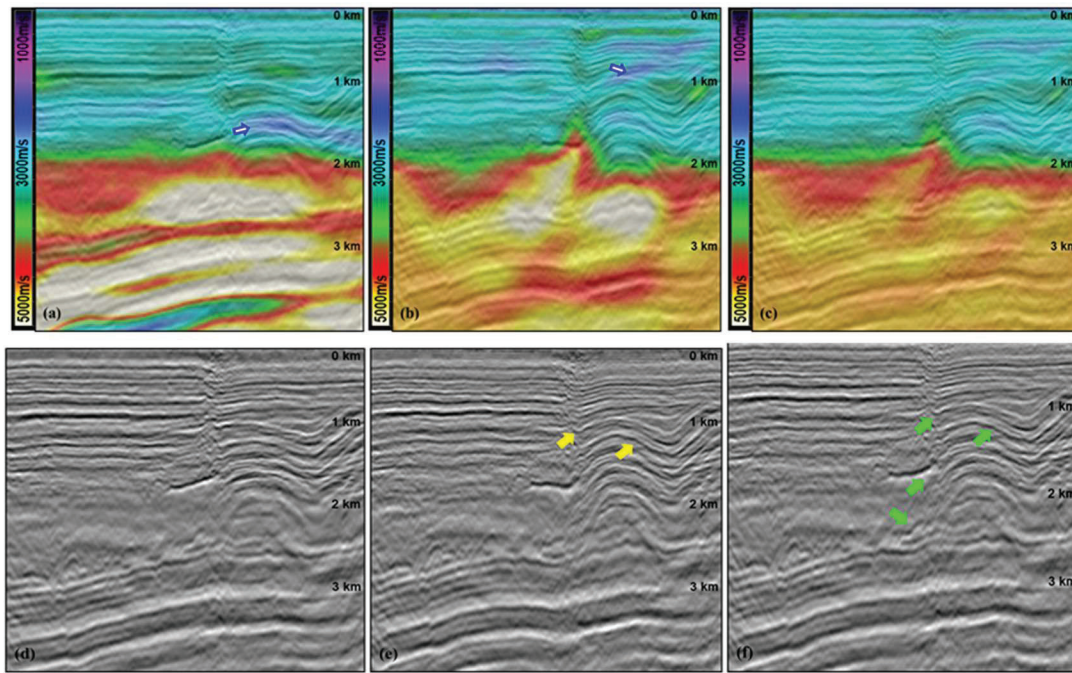


Figure 6 P-wave velocity model and corresponding RTM stack image: (a & d) after multi-layer tomography, (b & e) after 7 Hz LS-FWI, and (c & f) after 7 Hz multiD OT-FWI.

Conclusion

We have successfully implemented a cascaded flow of MWI and multiD OT-FWI to mitigate the geophysical challenges caused by Southern Oman's complex geology. MWI allows delineation of the sharp anhydrite layer and subsequent shallow velocity inversion of the Rus formation, which is vital to account for the presence of short-period internal multiples in the initial FWI forward model. By being less sensitive to amplitude errors, multiD acoustic OT-FWI proves to be more robust to cycle skipping in the presence of short period multiples and provides a more stable update, even beyond the maximum depth of penetration of the diving waves.

Acknowledgements

We would like to thank Occidental Petroleum and the Ministry of Oil and Gas of the Sultanate of Oman for permission to present the data examples. We also thank CGG for permission to publish these results.

References

- Bardainne T., [2018], Joint inversion of refracted P-waves, surface waves and reflectivity. 80th EAGE Conference & Exhibition, We K 02.
- Masclet, S., Bardainne, T., Massart, V., and H. Prigent [2019] Near surface characterization in Southern Oman: Multi-Wave Inversion guided by Machine Learning. 81st EAGE Conference and Exhibition, EAGE, Expanded Abstracts, 1528.
- Métivier, L., Brossier, R., Mérigot, Q., Oudet, E. and Virieux, J. [2016] Measuring the misfit between seismograms using an optimal transport distance: Application to full waveform inversion. *Geophysical Journal International* 205, 345-377.
- Perez Solano C. and Plessix R.E. [2019] Velocity model building with enhanced shallow resolution using elastic waveform inversion – An example from onshore Oman. *Geophysics*, 84, 6.
- Sedova, A., J. Messud, H. Prigent, S. Masclet, G. Royle, G. Lambaré [2019] Acoustic Land Full Waveform Inversion on a Broadband Land Dataset: the Impact of Optimal Transport. 81st EAGE Conference and Exhibition, EAGE, Expanded Abstracts, Th R08 07.